ACS APPLIED MATERIALS & INTERFACES

Research Article

www.acsami.org

Laser Ablative Surface Treatment for Enhanced Bonding of Ti-6Al-4V Alloy

Frank L. Palmieri,*[,†] Kent A. Watson,[†] Guillermo Morales,[‡] Thomas Williams,[§] Robert Hicks,[§] Christopher J. Wohl,[⊥] John W. Hopkins,[⊥] and John W. Connell[⊥]

[†]The National Institute of Aerospace, Hampton, Virginia 23666, United States

[‡]NASA Langley Research Summer Scholar, Hampton, Virginia 23681, United States

[§]University of California, Los Angeles, California 90095, United States

[⊥]NASA Langley Research Center, Hampton, Virginia 23681, United States

ABSTRACT: Adhesive bonding offers many advantages over mechanical fastening, but requires certification before it can be incorporated in primary structures for commercial aviation without disbond-arrestment features or redundant load paths. Surface preparation is widely recognized as the key step to producing robust and predictable adhesive bonds. Surface preparation by laser ablation provides an alternative to the expensive, hazardous, polluting, and less precise practices used currently such as chemical-dip, manual abrasion and grit blast. This report documents preliminary testing of a surface preparation technique using laser ablation as a replacement for the chemical etch and abrasive processes currently applied to Ti-6Al-4V alloy adherends. Surface roughness and surface chemical composition were characterized using interference microscopy and X-ray photoelectron spectroscopy, respectively. A technique for fluorescence visualization was developed which allowed for quantitative failure mode analysis. Wedge crack extension testing in a hot, humid environment indicated the relative effectiveness of various surface treatments. Increasing ablation duty cycle reduced crack propagation and adhesive failure. Single lap shear testing showed an increase in strength and durability as laser ablation duty cycle and power were increased. Chemical analyses showed trends for surface chemical species, which correlated with improved bond strength and durability.

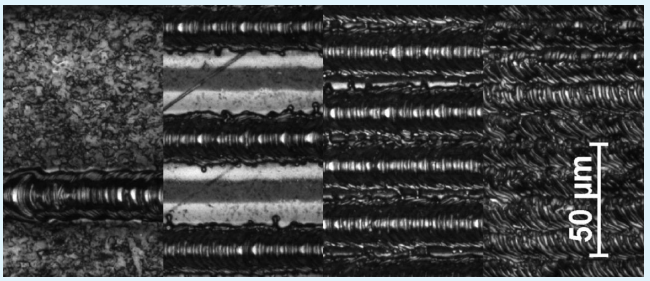

KEYWORDS: *Adhesion, Failure mode, Roughness, X-ray photoelectron spectroscopy (XPS), lap shear, PETI-5*

INTRODUCTION

Aircraft manufacturers rely increasingly on adhesive bonds to simplify airframe design and improve aircraft performance. Metal to composite bonds are becoming more common as the composite content of an aircraft is increased.[1] Replacing mechanically fastened joints with adhesive bonds can reduce weight, simplify manufacturing, and provide a stronger, more reliable joint, but solely bonded joints are not implemented in the primary structures of commercial aircraft because of predictability concerns and the inability to nondestructively assess bond strength. Restrictions on the application of adhesively bonded joints stem from a lack of control in current bonding methods.[1,2] New surface preparation methods, which promise to improve repeatability, minimize waste, and reduce costs, are under extensive evaluation by aircraft manufacturers.

The premature or unexpected failure of an adhesive bond can usually be traced to defects in the preparation of the faying surface.[3,4] Current surface treatment techniques based on mechanical abrasion such as grit blasting or sanding have limited repeatability and can leave contamination that reduces bond performance. State-of-the-art methods for modifying the surface chemistry of titanium alloys depend on wet chemical etchants containing acids, caustics, and oxidizers, usually in combination.[5−7] Such processes are expensive to perform because they are dangerous, create large volumes of hazardous waste, and are difficult to automate. The automation of surface preparation, which increases reproducibility, may be necessary for the certification of bonded primary structures.[1]

Nonstandard techniques such as atmospheric pressure plasma, arc discharge, and laser ablation have been demonstrated, but are still undergoing evaluation by the aerospace industry.[8−10] Laser ablation is a subtractive process which relies upon highly focused laser radiation to remove and redistribute material on a surface.[11−14] Ultraviolet laser systems are commonly used for high precision work such as medical procedures, the machining of fine parts, and printing microelectronic circuit patterns. The ablation process has been demonstrated to generate high precision surface topography simultaneously with the removal of surface contaminants and modification of surface chemistry.[15,16] Previous work by this

Received: October 11, 2012
Accepted: January 14, 2013
Published: January 14, 2013

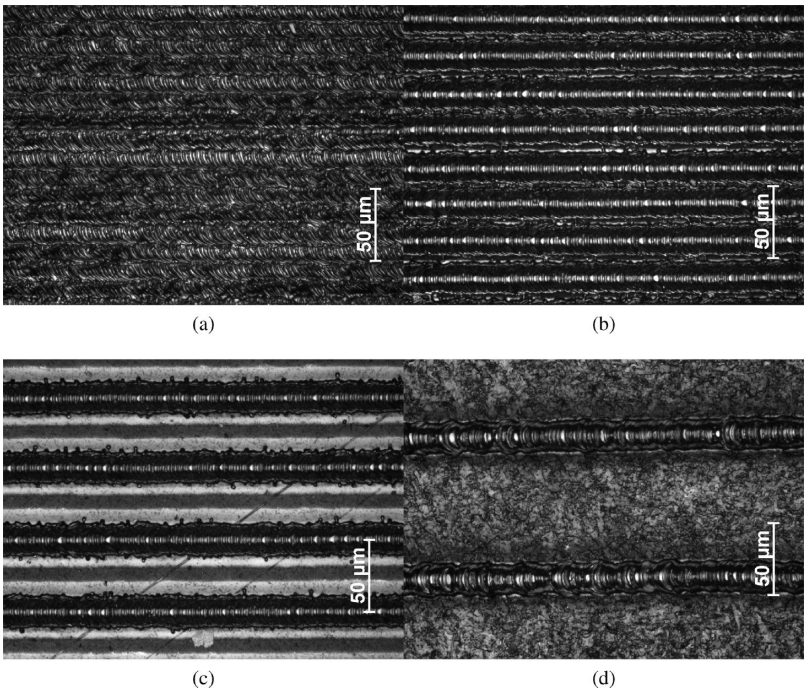

Figure 1. Parallel lines ablated into a Ti-6Al-4V surface with a pitch of: (a) 0.013 mm (0.0005 in.), (b) 0.025 mm (0.001 in.), (c) 0.051 mm (0.002 in.), and (d) 0.102 mm (0.004 in.).

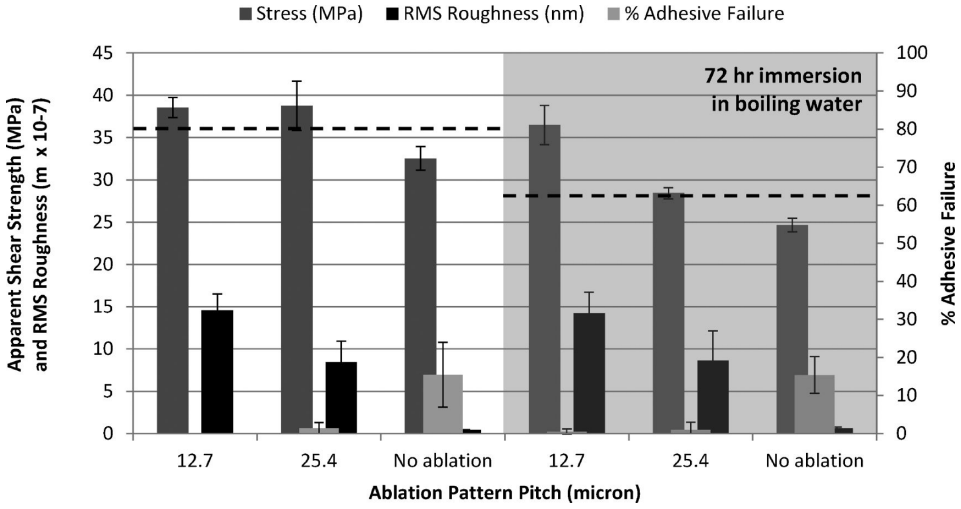

Figure 2. Results for SLS specimens prepared with polished adherends. Laser power was 1 W for all ablated specimens. Data in the shaded region was collected from specimens that underwent a 72 h immersion in boiling water immediately prior to testing. Dashed lines indicate the highest apparent shear strength values measured for SLS specimens that were not polished but were ablated. (1×10^{-7} m = 0.1 μm).

group demonstrated the utility of laser ablation to modify surface energy of titanium adherends using multifluid contact angle goniometry.[17]

This report presents the development of a laser ablation technique for the preparation of Ti-6Al-4V alloy faying surfaces. A neodymium doped yttrium aluminum garnet (Nd:YAG) laser that has been frequency tripled to a wavelength of 355 nm was used to clean/descale, create topographical patterns, and modify adherend surface chemistry prior to bonding with PETI-5 adhesive. The state-of-the-art processes that have been replaced include acid etching, caustic etching, grit blasting, and priming. A subset of the mechanical test specimens were polished before laser ablation processing to provide a starting surface free from native roughness and mill scale. Polished surfaces provided differentiation between ablation induced topography and native roughness. Macroscopic bond properties for a variety of lasing conditions were surveyed using wedge crack extension and single-lap shear (SLS) tests. The results were correlated with surface roughness measured by interferometric microscopy and surface chemistry characterized by X-ray photoelectron spectroscopy (XPS).

RESULTS AND DISCUSSION

Ablated Surface Properties. Laser ablation resulted in highly reproducible topography in the Ti-6Al-4V surface, as shown in Figure 1. The ablated specimens in Figure 1 are all patterned with parallel lines of various center-to-center spacing (pitch). The fraction of the total surface area ablated by the

beam is described by the ablation duty cycle. Duty cycle (d) is given by the ratio of the beam width (25.4 μm) to line pitch (p) such that d = (25.4 $\mu m/p$) × 100%. A duty cycle of 100% indicates that the entire surface was directly exposed to laser irradiation.

Adherends were laser processed both as-received and immediately after polishing. RMS roughness of the surface, as measured on an interferometric microscope, varied between 50 nm for highly polished surfaces, to 630 nm on the as-received surface, to about 1300 nm for heavily ablated surfaces. The effect of pattern density and power on roughness was observed by varying the pitch from 0.005 to 0.101 mm (0.2 to 4 mil), (500% to 25% duty cycle) at a constant power of 1 W and varying power between 200 and 1000 mW at a constant pitch of 25.4 μm (1 mil), respectively. The root-mean-square (RMS) roughness is reported with single-lap shear test results in Figures 2−4.

Single-Lap Shear Tests. The mechanical test results for polished SLS specimens that were ablated at 1 W are shown in Figure 2 along with roughness and failure mode statistics. Laser ablated specimens showed improvement in bond strength and predominantly cohesive failure mode in the adhesive as the pitch of the ablation pattern was reduced both before and after immersion in boiling water for 72 h. This supported the hypothesis that laser ablation improves the strength and durability of the titanium alloy/PETI-5 interface. The dashed lines in Figure 2 show the highest apparent shear strength achieved for unpolished specimens with optimal laser ablation treatment both before and after 72 h of immersion in boiling water.

Faying surfaces of adherends were polished before laser processing to provide a smoother starting surface than the inherently rough surface of the as-received adherends. The intention was to isolate the effects of laser generated topography on bond performance from the effects of native surface roughness by providing a smooth baseline (RMS roughness of 50 nm). The surface roughness and apparent shear strength of the specimens in Figure 2 show a strong, direct correlation which demonstrates the benefit of a roughened surface for bonding. Even though RMS roughness increased by more than 2 orders of magnitude, the apparent shear strength increased by less than 50% for samples immersed in boiling water and less than 20% for unaged samples. In addition, polished specimens without laser ablation were significantly stronger than specimens receiving neither polishing nor laser ablation processing (not shown, apparent shear strength: 16.5 MPa). These surprising results indicated that the polishing process increased bond strength primarily through surface chemistry modification, removal of contamination and stripping weakly bonded surface oxide layers. Thus, the effects of changing surface topography could not be isolated from surface chemistry variation through a polishing technique. Additionally, polishing is a slow, manual process which would be difficult to automate in a manufacturing environment; therefore, the polishing step was removed from subsequent experiments.

Lap shear test results for unpolished specimens which received laser surface preparation are summarized in Figure 3 showing trends for apparent shear strength, failure mode, and RMS roughness as the ablation line pitch is varied. Table 1 presents Pearson's correlation values for the unaged specimens shown in Figure 3. Pearson's correlation indicates a strong direct and indirect relationship between two variables for values

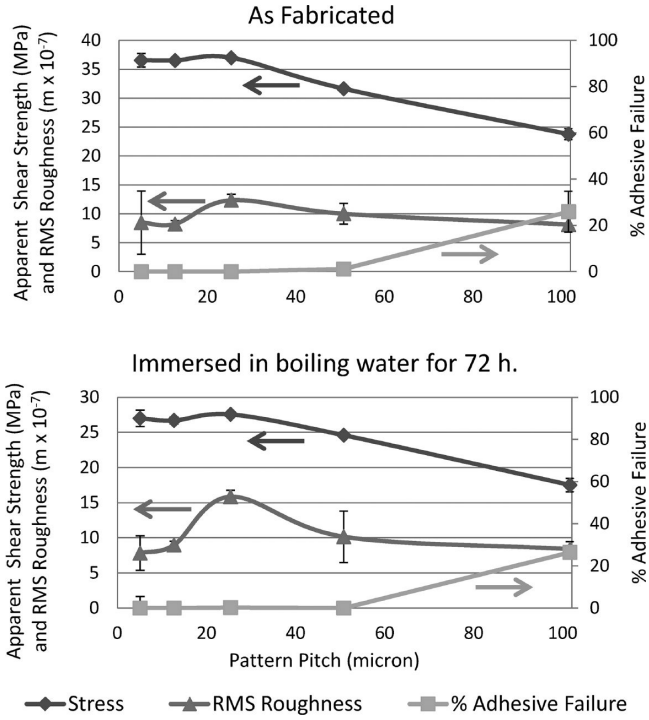

Figure 3. Apparent shear strength, failure mode, and roughness results for nonpolished adherends are shown for two data sets: variation of ablation line pitch without (top) and with (bottom) immersion in boiling water. (1×10^{-7} m = 0.1 μm).

Table 1. Pearson's Correlation Coefficients for Lap Shear Specimens with Varying Ablation Pitch (No Aging)

	strength	roughness	adhesive failure
pitch	−0.97	−0.28	0.87
strength		0.48	−0.87
roughness			−0.36

of 1 and −1, respectively, whereas a value of 0 indicates no correlation. Decreases in apparent shear strength correlate well with increases in adhesive failure mode, as anticipated. Laser ablation pitch appears to play a key role in maintaining an adhesive bond and driving the specimen to a cohesive failure mode. As the ablation duty cycle fell below 100%, bond properties immediately began to decline in sample sets with and without immersion in boiling water. After 72 h immersion in boiling water, mechanical tests showed about 25% loss in apparent shear strength but no significant change in failure mode. This indicated that immersion in boiling water for 72 h did not weaken the adhesive/metal interface, but degraded the properties of the cured PETI-5 adhesive. Capillary ingression of water along the glass fiber scrim cloth is suspected on the basis of the speed and magnitude of the property loss.

In Figure 3, RMS roughness is a maximum for a pitch of 25 μm (1 mil), which corresponds to a duty cycle of about 100%. The increase in roughness as the pitch decreases from 200 to 25 μm can be attributed to reduced space between the ablation trenches. At a pitch of 25 μm the ablation trenches are separated only by a very narrow line of unablated material as seen in Figure 1, b. This "sawtooth-like" pattern has greater roughness than any parallel line array with greater pitch. As the pitch is further reduced, the trenches overlap one another to form a single ablation field, which removes the large

topographical variations from between the trenches. The apparent shear strength has a maximum value at the same pitch as the peak in RMS roughness which indicates that increasing roughness improves strength. As observed for polished specimens, the large changes in RMS roughness (100%) correlate to small changes in apparent shear strength (5%).

The data shown in Figure 4 and Table 2 present strong correlations between bond performance and laser power. The

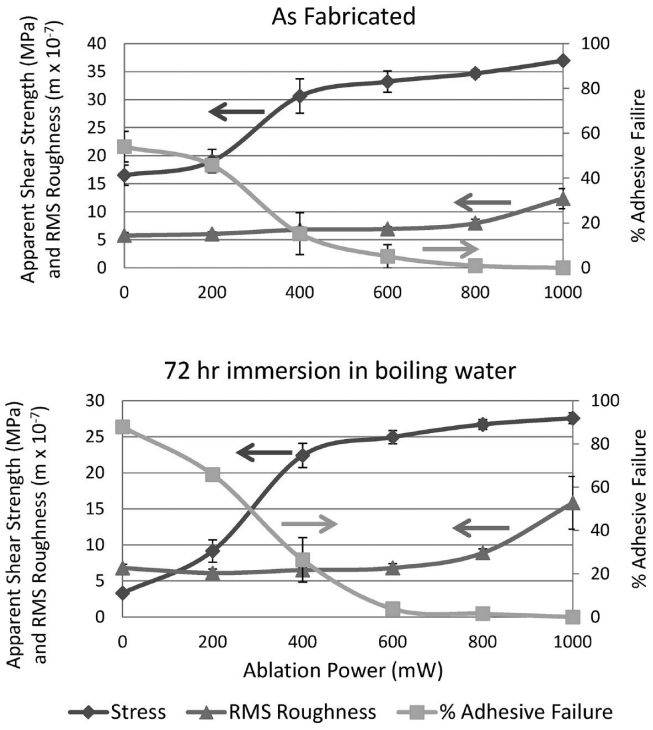

Figure 4. Roughness and lap shear data for nonpolished, laser ablated adherends are shown for two data sets: laser power variation without (top) and with (bottom) immersion in boiling water. (1×10^{-7} m = 0.1 μm). Ablation pitch was 25.4 μm for all specimens.

Table 2. Pearson's Correlation Coefficients for Lap Shear Specimens with Varying Ablation Power (No Aging)

	strength	roughness	adhesive failure
power	0.94	0.85	−0.93
strength		0.71	−1.00
roughness			−0.66

apparent shear strength increases dramatically, and the failure mode switches to cohesive failure as the ablation power is increased. The same trend is also observed for specimens immersed in boiling water for 72 h although correlation coefficients are not presented for brevity. Bond improvement appears to plateau at about 800 mW of laser power, which coincides with the adhesive failure mode reaching nearly 0%.

The RMS roughness of the ablated surface does not significantly increase relative to the roughness of the native titanium alloy surface for laser powers less than 800 mW. Apparent shear strength increases dramatically between 200 and 400 mW of ablation power while the apparent shear strength above 400 mW of laser power increases slowly. These two observations, taken together, indicate that laser ablation at relatively low power has a profound effect on surface chemistry with minor effect on surface topography. The changes in surface chemistry cause the significant improvement seen in apparent shear strength and failure mode that is seen below 400 mW ablation power. As the surface roughness increases steeply between 600 and 1000 mW laser power, improvements in bond properties are less significant. These findings support previous observations that surface roughness is a secondary factor influencing the bond strength of a lap shear specimen prepared by laser ablation. Similar results have been observed by others using alumina grit blasting to roughen titanium alloys.[18]

Wedge Crack Extension Tests. Wedge tests provide an excellent, semiquantitative comparison of surface preparations by applying a mode I opening stress in a hot wet environment, but unlike other mode I mechanical tests, such as the double cantilever beam test, wedge tests are relatively inexpensive to prepare and conduct. Combination of the wedge test method with a precision failure mode inspection technique such as the fluorescence visualization technique presented here provides a quantitative means for failure analysis. Accurate characterization and distinction of different surface preparations is possible using these techniques.

The polishing process was not performed during the preparation of wedge test samples. Based on lap shear test results, a reduced set of laser parameters were selected for wedge test experiments as shown in Table 3 in order of

Table 3. Laser Parameters Used for Preparation of Wedge Test Adherend Surfaces

	sample		
	A	B	C
fluence (J/cm^2)	5	8	20
power (mW)	1000	400	1000
pitch (μm)	100	25	25
duty cycle (%)	25	100	100

increasing laser fluence. Specimen A received the optimum power for maximum bond performance, but the pitch was increased to reduce the duty cycle. Specimen B received the optimal line pitch but at a reduced power expected to give good surface chemistry but only minimally affect surface roughness. Specimen C received the optimum laser power and line pitch for maximum bond performance.

The crack extension after 24 h of aging and the percent adhesive failure data for the samples are shown in Figure 5.

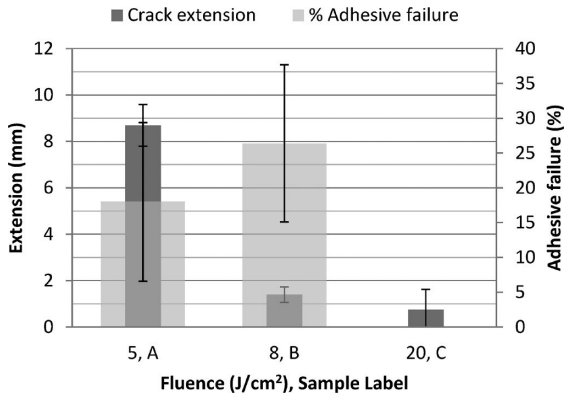

Figure 5. Crack extension and failure mode data for wedge test specimens ablated with three different laser fluence levels.

dx.doi.org/10.1021/am302293m | ACS Appl. Mater. Interfaces 2013, 5, 1254−1261

Wedge tests supported the conclusions drawn from lap shear testing to determine the optimum laser ablation surface preparation. Specimen A was expected to perform poorly based on comparisons with lap shear data with the same duty cycle. A 25% duty cycle leaves about 75% of the faying surface untreated and therefore a poor bond results even though the laser power was optimized at 1 W. Crack extension in specimen A was greater than that for specimens B and C. The appearance of adhesive failure in specimen A also supported the hypothesis. On the basis of lap shear results, specimen B was expected to be similar to specimen C because moderate laser power at 100% duty cycle produces the necessary chemical modification over the entire surface for good bond performance. Crack extension was extremely low like that of specimen C, and adhesive failure mode was moderate which matches lap shear results. Specimen C exhibited no adhesive failure mode and minimal crack growth after 24 h of aging. This result reinforces the observation that a high duty cycle is most important for good bonding, and best results are achieved when the power is high enough to achieve full chemical modification of the surface (to be discussed) and increase surface roughness. The large error bars for failure mode data in Figure 5 are attributed to sample fabrication issues. The adhesive did not flow and wet the edges of 15 cm (6 in.) by 20 cm (8 in.) panels as well as the center region, and therefore edge specimens exhibited higher values for adhesive failure mode and greater crack extension than specimens cut from the center of the panel.

XPS Analysis. Unpolished titanium adherends were ablated at a 25.4 μm pitch with power variation between 0 and 1000 mW before interrogating the surface using XPS. Survey scan data are presented in Figure 6 for select elements. Shaded areas indicate the dominant failure modes observed during SLS testing. Constituents such as carbon, nitrogen and silicon appeared in the XPS spectra, but were removed from the data analysis. It is believed that these elements played no role in bonding, and they were introduced as surface contaminants after ablation but before XPS inspection.

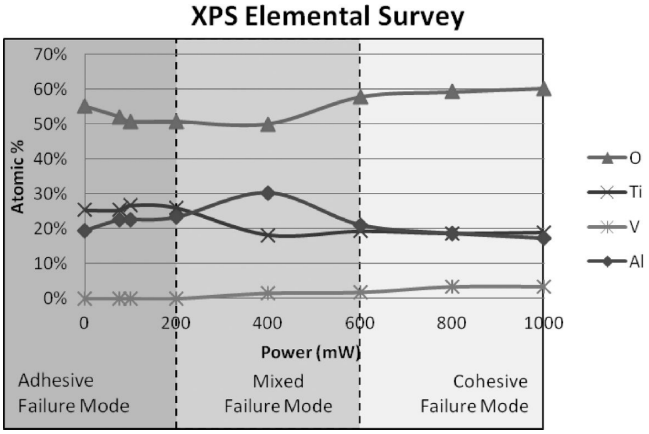

Figure 6. XPS survey scan data showing the atomic percent abundance of select elements found in survey scan spectra. Shading on the figure indicates the dominant failure mode seen in SLS test specimens.

The survey scan data in Figure 6 indicate changes in elemental abundance at the adherend surface that correlate with changes in the observed failure mode. At low laser ablation powers, oxygen abundance decreases while aluminum and titanium abundances increase. This may indicate the removal of surface oxides and mill scale. At ablation powers greater than 400 mW, vanadium begins to appear at the surface and the abundance of oxygen increases. The appearance of vanadium on the surface is likely due to surface material ablation which exposes the underlying, bulk alloy. The increase in oxygen concentration is attributed to the oxidation of the surface metals and suboxides. At greater than 400 mW, the surface concentrations of titanium and aluminum decreased slightly because of dilution by vanadium and oxygen as the ablation power was raised.

Little correlation was seen between the elemental composition of the surface and the failure mode of the adhesive; however, the bonding states of each element must also be considered. Deconvolution of the $Ti2p_{1/2}$, $Ti2p_{3/2}$, O1s, and Al2p multiplex peaks was performed on high-resolution XPS spectra and peak assignments were made as shown in Figure 7. Figure 8 summarizes the surface composition data for each of the metals and oxides found on the alloy surface after ablation. Shading on the figure indicates the dominant failure mode observed in three power ranges based on the SLS failure mode results. The concentration of titanium dioxide increased steeply between 200 mW and 400 mW of laser power while all other titanium constituents diminished in concentration. This is consistent with the increased atomic percentage of oxygen observed in Figure 6. It also indicates that laser ablation at higher power causes oxidation, which has been linked to improved bond performance.

The deconvolution of the XPS spectra in Figure 7 shows that oxygen was found in five different chemical species on the adherend surface though none of them appeared to change dramatically across the range of laser power explored. The removal of the more highly oxidized hydroxyl species ($-(OH)_{OX}$) is thought to improve bond performance based on previous work.[19] Deconvolution of the aluminum multiplex revealed two components: aluminum metal and alumina (Al_2O_3). Between 200 mW and 400 mW of laser power, the aluminum metal was quickly oxidized to alumina which coincided with changes in bond performance. The correlation of these XPS results with SLS data in Figure 4 indicate strongly that formation of new titanium and possibly aluminum oxide layers on the surface contributes significantly to bond performance. The surface oxidation produced by laser processing appears similar to that produced by state-of-the-art, chemical-dip processes such as Turco 5578, which also forms a stable layer of titanium dioxide and suboxides.[6,7,20]

Based on the XPS and SLS results, parallel lines ablated at greater than 400 mW power and at 25 μm pitch produce high surface concentrations of titania and alumina which, when bonded with the PETI-5 adhesive, formed robust bonds with apparent shear strengths and failure modes comparable to current state-of-the-art surface preparation techniques.[21] Surfaces prepared by laser ablation resulted in 100% cohesive failure which is a necessary attribute of bonded materials. The apparent shear strength results presented here are not compared with literature values directly because changes in bondline thickness, adhesive preparation, and bonding processes can cause large variations in test results. Wedge tests and SLS tests both indicate that maximizing roughness improves bond performance, but has less significant impact than surface chemistry modification. Laser ablation surface preparation was demonstrated as a viable alternative to current surface preparation methods to achieve high bond strength and durability. Laser processing is inherently high precision and capable of providing a repeatable surface preparation. In

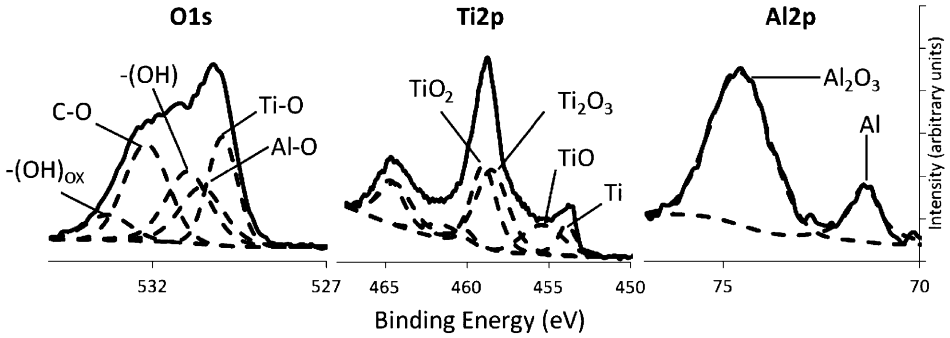

Figure 7. Deconvolution of a high-resolution O1s, Ti2p, and Al2p spectra from different specimens showing peak assignments.

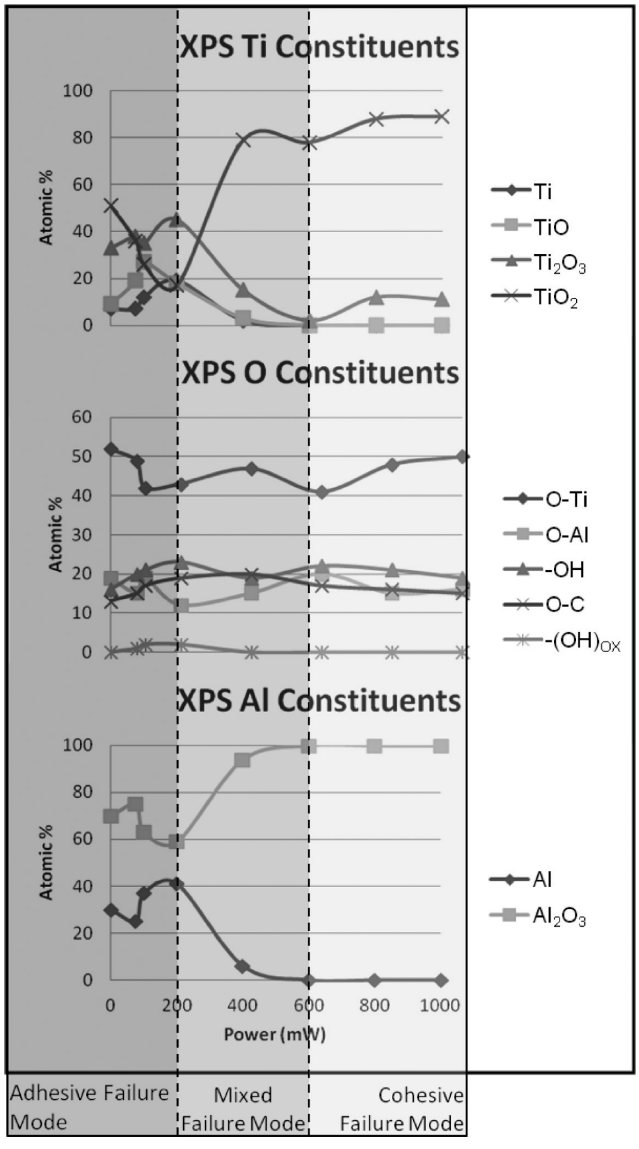

Figure 8. Atomic percent abundance of surface constituents based on the deconvolution of the Ti2p1/2 and Ti2p3/2 mulitplex (top), O1s peak (center), and Al2p peak (bottom). Shading on the figure indicates the dominant failure mode seen in SLS test specimens.

addition, laser ablation provides an alternative, green means of surface preparation on titanium adherends by avoiding the use of toxic chemicals and etchants.

EXPERIMENTAL SECTION

Materials and Methods. Titanium alloy for single-lap shear testing (Ti-6Al-4V, an alloy consisting of 90% titanium, 6% aluminum and 4% vanadium, 1.6 mm [0.063″] thick) was purchased from California Metal & Supply, Inc. and supplied in the configuration shown in Figure 9. This configuration is a modification of specimens

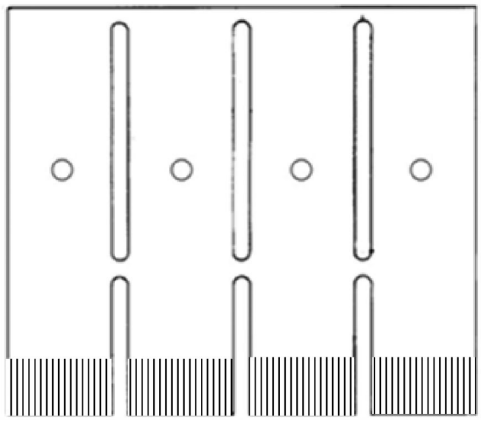

Figure 9. Modified single-lap shear adherend geometry indicating laser-etched portion.

called for in ASTM D1002−05, and allowed for the use of an existing bonding jig. Titanium alloy for wedge test specimens was purchased from the same vendor with a thickness of 3.18 mm (0.125″) in a configuration specified by ASTM D3762−03.

Phenylethynyl-terminated imide (PETI) high temperature adhesive, PETI-5 (2500 g/mol), was chosen for these experiments based on this laboratory's extensive experience with polyimide adhesives. The synthesis of PETI-5 was conducted in-house, and is described elsewhere.[22] Optical micrographs were taken with a Zeiss Exciter microscope equipped with a Zeiss Axiocam digital camera. Roughness was measured using a New View 6000 optical surface profiler from the Zygo Corporation equipped with a 2.5× objective and a 1× zoom tube. XPS was performed on a ThermoFisher ESCAlab 250 X-ray photoelectron spectrometer.

Polishing of Titanium Adherends. A Buehler Ecomet III with an Automet head and 300 mm platen was used to polish a subset of samples to a RMS roughness of 0.050 ± 0.010 μm across the faying surface. The native RMS roughness found on the faying surface of titanium alloy lap shear substrates before polishing was 0.630 ± 0.030 μm. Polishing was performed in stages starting with 240 grit silicon carbide paper via wet-sanding and progressing through 320, 400, 600, 800, and 1200 grit papers. The final polish was performed on a velpol polishing cloth using slurry made from 0.05 μm colloidal alumina, water, and alkaline, liquid detergent in about equal parts. Lower platen polishing speeds were maintained between 100 and 150 rpm, and the downward force of the head was between 44.5 and 222 N (10 and 50 lbs).

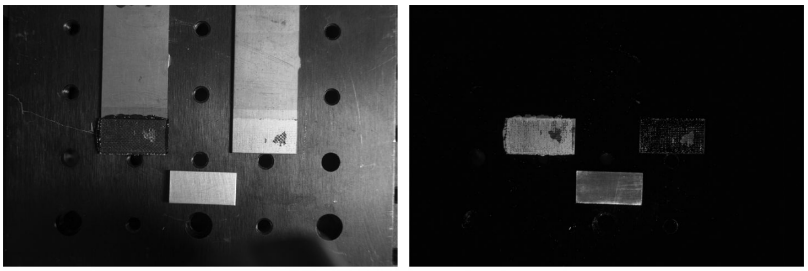

(a) (b)

Figure 10. On the left is a visible light image of a failed lap-shear specimen showing mostly adhesive failure. On the right is a fluorescence image of the same specimen with clearly visible adhesive residues. A 12.7 mm × 25.4 mm (0.5 in. × 1 in.) reference standard with a fluorescent coating is visible at the bottom of each image.

Preparation of Adhesive Tape. PETI-5 (2500 g/mol) adhesive tape was prepared in-house and used for bonding all specimens. An E-glass scrim cloth (style 112, A-1100 finish, 2-ply twisted yarn in a 0°/90° plain weave, 0.09 mm thick, γ-aminopropyl silane treated) was stretched onto a 22.5 cm × 32.5 cm frame. The scrim cloth was impregnated with adhesive by brushing on a solution of PETI-5 poly(amic acid) adhesive in N-methyl-2-pyrrolidinone (NMP). Initial coats were made with an 8 wt % solution of PETI-5 oligomer in NMP solvent, and were continued until a nonporous tape was formed (4 to 8 coats). Subsequent coats were applied at 20 and 30 wt % to build the tape thickness to 0.30 mm (12 mil; 15−20 coats). After each coat was applied, excess NMP was removed by heating the tape in stages to a final temperature of 230 °C.

Laser Ablation. Laser ablation of Ti-6Al-4V coupons was performed on a PhotoMachining, Inc. laser ablation system with a Coherent, Avia frequency tripled Nd:YAG laser (7 W nominal pulsed output at 355 nm). Single lap shear specimens were ablated with parallel lines on the faying surface using a direct write process. The lines were oriented along the length of the specimen so that the ablation pattern was parallel to the tensile load during the mechanical test as indicated in Figure 9. The write speed (25.4 cm/s) and pulse frequency (80 kHz) were held constant for all experiments. The pattern density was varied by changing the pitch of the parallel lines, and the laser power was varied and monitored after the final lens element using a thermopile sensor (model 3A-SH) and Nova II power meter from Ophir Spirocon LLC. Throughput of the laser system was not optimized in this study, but the experimental processing rate ranged from about 32 to 1.3 cm^2/min depending on pattern density.

Bonding. Mechanical test specimens were bonded in a 30 cm ×30 cm, heated Carver press for 1 h at 371 °C and 0.34−0.68 MPa (50 - 100 psi). For single-lap shear specimens, bonding configurations were shimmed to maintain a 0.13 ± 0.025 mm (0.005 ± 0.001 in) bondline thickness. Wedge test samples were bonded by aligning two 15 cm by 20 cm titanium alloy plates in a jig with a 15 cm by 17.5 adhesive film and a 15 cm by 2.5 cm precrack film held between them. Shims were not required to maintain the minimum bondline thickness for wedge tests. Samples were compressed and held at full load beginning at room temperature and until after the press cooled below 150 °C. Compressed air was used to speed the cooling process.

Mechanical Testing. Single-lap shear specimens were tested according to ASTM D1002−05 using a mechanically actuated test frame manufactured by Measurement Technology Inc. equipped with a 22.2 kN (5 kip) load cell and pin fixtures. Four specimens were tested for each set of experimental conditions. Additional lap shear specimens were subjected to a 72 h water boil according to ASTM D1151−00 immediately prior to testing. All specimens were tested at room temperature.

After bonding, wedge test samples were machined into 25.4 mm wide specimens using an abrasive water jet cutting tool to avoid heating. Five specimens were tested for each set of experiments conditions. Bondline thickness was measured optically by viewing the cross-section of each specimen on both sides. Wedge specimens were opened by forcing an aluminum wedge into the precrack end according to ASTM D3762−03. The initial crack length was marked immediately before specimens were introduced to the aging chamber one hour after wedge insertion. Aging conditions were 60 °C and 100% relative humidity, which were maintained by placing a desiccator partially filled with water into an oven. Specimens were placed on a shelf in the desiccator in the head space over the water. Specimens were removed to mark the crack tip position after 1, 8, 24, and 48 h and 1, 2, and 4 weeks.

Fluorescence Failure Mode Analysis. The failure mode of each specimen was determined using a fluorescence visualization technique based on the fluorescent properties of the PETI-5 adhesive in contrast to the nonfluorescent metal adherends. Gray scale, digital images of each adherend were collected using a Kodak DCS-760 M camera with cold cathode detector and a LM2X-DM LED ultraviolet light source from Innovative Science Solutions Inc. having a peak output wavelength of 400 nm. A Kodak, orange gelatin filter was used to prevent reflected light from reaching the camera detector. Example images of a failed lap shear specimen under visible and UV illumination, respectively, are shown in Figure 10. The small rectangle seen at the bottom is a size reference machined from aluminum and stained to be visible under fluorescent conditions. The contrast between adhesive-covered and adhesive-barren areas allows for the use of Image J software to count the number of pixels in the bondline with no adhesive present. Each image was aligned, the failure surface region was selected and a binary threshold was applied to distinguish fluorescent from dark pixels. The percentage of surface area lacking adhesive was taken as the percentage of adhesive failure. With careful image collection and image analysis, the error for this technique was determined to be 1.2%.

AUTHOR INFORMATION

Corresponding Author

*E-mail: frank.l.palmieri@nasa.gov.

Notes

The authors declare no competing financial interest.

ACKNOWLEDGMENTS

The authors thank Dr. Tony Belcher and Dr. Kay Blohowiak of The Boeing Company for their insightful technical discussions, recommendations, and review of this manuscript. Dmitry Pestov and Everett Carpenter at Virginia Commonwealth University are acknowledged for providing XPS services and related technical advice. Finally, thanks are due to Thomas Jones from the NASA Langley Research Center for constructing the apparatus used for fluorescence visualization of failed mechanical specimens.

REFERENCES

(1) Bossi, R.; Piehl, M. *Manuf. Eng.* **2011**, *59*, 101−109.
(2) Perton, M.; Blouin, A.; Monchalin, J.-P. *J. Phys. D: Appl. Phys.* **2011**, *44*, 12−22.
(3) Davis, G. *Surf. Interface Anal.* **1993**, *20*, 368−372.

(4) Davis, M.; Bond, D. *Int. J. Adhes. Adhes.* **1999**, *19*, 91−105.
(5) Lui, H.; Simone, C.; Katiyar, P.; Scola, D. *Int. J. Adhes. Adhes.* **2005**, *25*, 219−216.
(6) Critchlow, G. W.; Brewis, D. M. *Int. J. Adhes. Adhes.* **1995**, *15*, 161−172.
(7) Cotter, J.; Mahoon, A. *Int. J. Adhes. Adhes.* **1982**, *2*, 47−52.
(8) Rechner, R.; Jansen, I.; Beyer, E. *Int. J. Adhes. Adhes.* **2010**, *30*, 595−601.
(9) Broad, R.; French, J.; Sauer, J. *Int. J. Adhes. Adhes.* **1999**, *19*, 193−198.
(10) Molitor, P.; Barron, V.; Young, T. *Int. J. Adhes. Adhes.* **2001**, *21*, 129−136.
(11) Baburaj, E.; Starikov, D.; Evans, S.; Shafeev, G.; Bensaoula, A. *Int. J. Adhes. Adhes.* **2007**, *27*, 268−276.
(12) Rotel, M.; Zahavi, J.; Tamir, S.; Buchman, A.; Dodiuk, H. *Appl. Surf. Sci.* **2000**, *154−155*, 610−616.
(13) Benard, Q.; Fois, M. G. M.; Lauren, P. *Int. J. Adhes. Adhes.* **2006**, *26*, 543−549.
(14) Benard, Q.; Fois, M.; Grisel, M.; Laurens, P.; Joubert, F. *J. Thermop. Compos. Mater* **2009**, *22*, 51−61.
(15) Belcher, M.; Wohl, C.; Hopkins, J.; Connell, J. Laser Surface Preparation and Bonding of Aerospace Structural Composites. In *55th International SAMPE Symposium and Exhibition*, Seattle, WA, 2010.
(16) Belcher, M. A.; Wohl, C. J.; Connell, J. W. Surface Preparation and Bonding of Composite Aircraft. In *32nd Annual Meeting of the Adhesion Society*, Savannah, GA , 2009.
(17) Belcher, M. A.; List, M. S.; Wohl, C. J.; Ghose, S.; Watson, K. A.; Hopkins, J.; Connell, J. W. Laser Surface Preparation For Adhesive Bonding Of Ti-6Al-4V. In *SAMPE Electronic Proceedings*, Seattle, WA, 2010.
(18) Harris, A.; Beevers, A. *Int. J. Adhes. Adhes.* **1999**, *19*, 445−452.
(19) Harris, E. W.; Massey, J. T.; Chen, D.; Williams, T.; Hicks, R. F.*Atmospheric Plasma Effects on Structural Adhesive Bonding*; technical paper presented at SAMPE11; Long Beach, CA, May 23−26, 2011 ; Society for the Advancement of Material and Process Engineering: , 2011
(20) Mertens, T.; Kollek, H. *Int. J. Adhes. Adhes.* **2010**, *30*, 466−477.
(21) Smith, J. G.; Connell, J. W.; Hergenrother, P. M. *J. Compos. Mater.* **2000**, *34*, 614−628.
(22) Hergenrother, P.; Connell, J.; Smith, J. *Polymer* **2000**, *41*, 5073−5081.